Study on a Compatible Model Combining Point Cloud Model and Digital Elevation Model

Wenbo Guo[1], Jun Zhao[1]

[1]College of Geography and Environment Science, Northwest Normal University, Lanzhou 730070, China

5 *Correspondence to*: Zhao Jun[1] (zhaojun@nwnu.edu.cn)

Abstract. DEMs(Digital Elevation Model) are important data sources that describe the surface morphology, but they are not real 3D models and thus cannot meet the requirements for describing the land surface in 3D. LIDAR(Light Deteation and Ranging) point cloud data are true 3D data with high precision and a high density. Based on an analysis of the differences between DEM and point cloud data, including the corresponding acquisition methods, data structures and model construction

10 methods, this paper proposes a 3D point set data model based on regular grid 2D data field for regional modeling. The feasibility of the model is tested through the upper and lower boundary modeling method. The experiments show that (1) the 3D point set data model based on regularly gridded 2D data field is compatible with complete DEM data and simplified point cloud data and has good applicability; (2) the newly built data model can be used in the true 3D modeling of simple surface entities with high efficiency when the amount of data is only doubled; and (3) the new data model can be generated

15 by inputting DEM data and point cloud data and using a simplified algorithm to process the point cloud data in the same coordinate system. This approach has the potential for multiscale, including large-scale, and automatic output processing and has the potential to be widely generalized.

1 Introduction

As important digital representations of the Earth's surface, digital elevation models (DEMs) have been around for half a

20 century (Hu and Cao, 2013). In a mathematical sense, a DEM is a digital simulation of the surface through a continuous function H = f (x, y) in 2D (two-dimensional) space. A DEM is not a real 3D (three-dimensional) model because geoscience data field are generally collected in 2D; thus, data are displayed in the real 3D environment, but descriptions of real 3D spatial entities are not available (Wang et al., 2003). The requirements for true 3D data are high in geoscience research (Li et al., 2016; Zhang et al., 2006; Zhou et al., 2018), and 2.5-dimensional DEM data cannot fully meet the current application

25 requirements. Under the condition that mainstream data sources cannot be abandoned, scholars have performed considerable research on the expression of DEM-based 3D geoscience data (Wang et al., 2003; Wu and Yu, 2012; Liu et al., 2010; Wang et al., 2019). A simple DEM cannot provide true 3D descriptions of complex objects such as karst caves, sinkholes, strata, and architectural structures. Only through multisource data fusion modeling can true three-dimensional modeling based on

DEMs be completed. Currently, borehole data are most commonly used (Duan, 2004). LIDAR point cloud data, as a new

30 type of high-precision, high-density true 3D data collected in recent years, provide a reliable 3D data source for indoor

positioning, 3D modeling, high-precision DEM production, etc. Such data have good application prospects in the

development of DEMs for true 3D modeling.

This paper attempts to establish a new data model that is compatible with simplified point cloud data and has the potential to

be used in large-scale and multiscale automatic true 3D processing while ensuring the integrity and simplicity of the DEM

35 data. The 3D data descriptions are considered to perform research involving complex terrain modeling, 3D Earth

representations, basic-level true 3D mapping and 3D city analysis.

2 Basic ideas and key technologies

2.1 Basic ideas

A data model includes the data structure, data operations and data constraints. The differences among data models associated

40 with different data structures are important sources of characteristic differences related to the use of DEM data and point

cloud data. The commonly used DEM formats include Virtuozo-DEM, CNSDTF-DEM, USGS-DEM, etc. (Li and Peng et al.,

2008). There are certain differences among various data formats, but the data storage concepts are basically the same. The

attributes of a regular grid are determined by the starting point, X-Y spacing and numbers of rows and columns in the header

file. The elevation values are arranged in the file according to certain rules. This approach uses a one-dimensional array for

45 the storage of a 3D point set. The USGS format is slightly different; this format stores row and column elevation data by

section and describes the spatial grid with an interval of seconds. However, the combination of a grid description and a

one-dimensional array is still utilized.

The data files recorded by LIDAR equipment are generally based on the Las format (Zhang et al., 2014) issued by the

LIDAR committee of the American Society for Photogrammetry and Remote Sensing (ASPRS). This format contains a large

50 number of parameters, such as coordinates, colors, laser return points, and scanning angle ranges. For ease of use, generally,

LAS-format point cloud data are converted into a variety of other more concise and easy-to-use formats for processing. At

present, the main simplification method for point cloud data is to dilute the point cloud through a certain algorithm.

By ignoring the header file, which contains a very small proportion of data, DEM data can be regarded as a matrix with X

rows and Y columns, where X=the total number of points and Y=the bytes in a single record. Correspondingly, point cloud

55 data can be regarded as a matrix with the number of rows X+$\triangle$x and the number of columns Y+$\triangle$y. Then, the difference

$\triangle$P between the point cloud data and the DEM data is Eq. (1):

$$\Delta P = (X + \Delta x) \cdot (Y + \Delta y) - X \cdot Y$$
$$= \Delta x \cdot \Delta y + \Delta x \cdot Y + \Delta y \cdot X \quad , \tag{1}$$

Currently, publicly available DEM data have grid resolutions of 90 and 30 meters, and the resolution of LIDAR data can reach the millimeter level. Additionally, the length of a single record of point cloud data is at least approximately 3 to 4 times

60 that of DEM data. Based on estimations with the above formula, in an equal area and for an equal recording accuracy, the data volume of point cloud data is approximately 9,000 to 360,000 times that of DEM data. Thus, there is a huge gap between the amount of DEM data and the amount of point cloud data stored.

Whether or not a data model can objectively describe an object in 3D depends on whether the data model supports the 3D data field. The 2D data field has limitations in the description of complex 3D volumes, and there is distortion in the

65 description of true 3D data with the same horizontal coordinates and multiple elevations. Therefore, a data model that is compatible with the two data types must consider data dimensionality reduction, point set thinning, and the support of true three-dimensional data.

2.2 Data modeling and management

Combined with the structure of DEM data and the multidimensional characteristics of point cloud data, this paper proposes a

70 regular grid point set data model. The single point form of the model is (X, Y, Z, O), in which X-Y are the horizontal coordinates, Z is the elevation value, and O is the supplementary dimension. The supplementary dimension can be expanded according to the specific case, but it should be consistent in a single model. A data model in which O is a one-dimensional identification dimension is provided below.
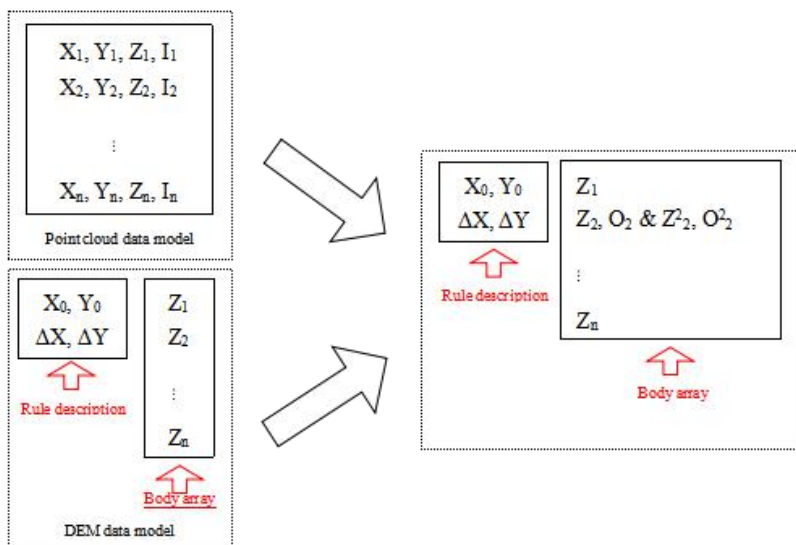
75   **Figure 1: Comparison of the structures of the point cloud data model, DEM datamodel and compatible data model**

As shown in Figure 1, X_0 and Y_0 represent the starting coordinates, $\triangle X$ and $\triangle Y$ represent the regular grid spacings, and I

encompasses the intensity and RGB color information contained in the point cloud data. The data dimension of I may be

greater than or equal to 1 depending on the research purpose and data structure. The compatible data model divides the data

into regular grid nodes and compresses the horizontal coordinate data based on the starting coordinates and rule descriptions.

80   Points with the same X-Y values are points in the same grid cell. In the same grid cell, there will be an odd number of

boundary points between a three-dimensional entity and an empty interval from the uppermost nonphysical space to an

elevation starting surface below the ground surface; therefore, each grid cell will store $2n+1$ elevation values. Taking Figure

2 as an example, when $n = 1$, the elevation points to be stored for grid point P are P_1, P_2 and P_3.
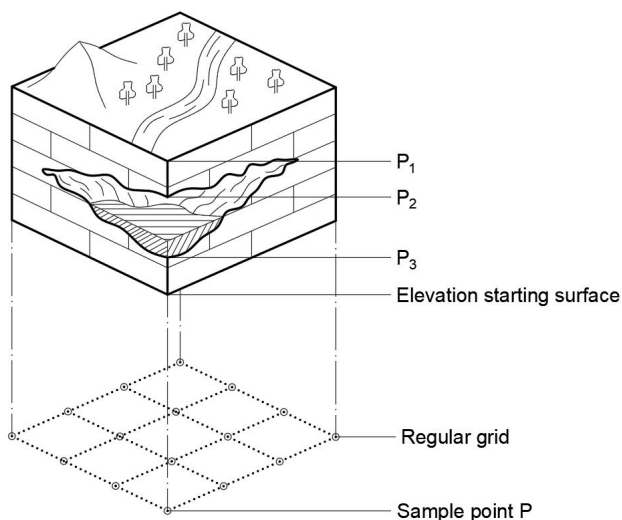
85   **Figure 2: Schematic diagram of compatible model identification points**

The number of elevation values corresponding to each 2D grid point (X_P, Y_P) in the compatible model is different than that

in the DEM and point cloud data models, so a one-to-many nonlinear structure should be adopted for data management.

Although the compatible model is essentially a set of fixed-dimension points, each text array needs to correspond to a certain

2D grid point coordinate when horizontal coordinate compression and decompression are performed; however, the same 2D

90   grid point coordinates may correspond to an indefinite number of body arrays.

2.3 3D solid modeling based on the compatible model

An independent point set without topological relations cannot completely describe 3D data, so establishing topological

relations and 3D solid models of points are tasks that must be performed to achieve true 3D modeling with compatible

models. Based on the applicability of a compatible model, the complementary dimension O of the compatible model can be

95 simply defined based on the upper and lower boundary identifiers of a 3D entity, where U is used to identify the upper bound of the 3D entity and L is used to identify the lower bound of the 3D entity. The points in the upper and lower bound model are numbered as 1, 2...2n + 1 (n ∈ N), where 2i + 1 is point U and 2i is point L. From top to bottom, the space from point U to point L and the space from point 2n+1 to the elevation plane are used to define the three-dimensional space where entities exist; the space from point L to point U and the space above point 1 are defined as a three-dimensional space without entities,

100 and the model is established based on these relations.

The topological relationships among the 3D point set do not exist only in the vertical direction. Because 2D data fields are used in DEM data sets, there is a one-to-one correspondence between the two points of nearest neighbors in the grid. However, in the compatible model, there may be 2i + 1 and 2j + 1 points in the adjacent 2D grid elements A and B, and the size relationship between i and j is uncertain, which makes it difficult to accurately establish the corresponding topological

105 relationships. In this paper, a regional modeling method is used to solve this problem. First, a region with equal points is independently modeled, and the points in the independent modeling area correspond to the grid serial numbers from top to bottom. Then, multiple 3D planes or surfaces based on a 2D data field can be established by interpolation, and a 3D solid model can be established according to the point layer identifiers of the 3D solid. After all independent modeling areas are considered, the 3D solid model of the region can be obtained by merging the submodels, as shown in Figure 3.
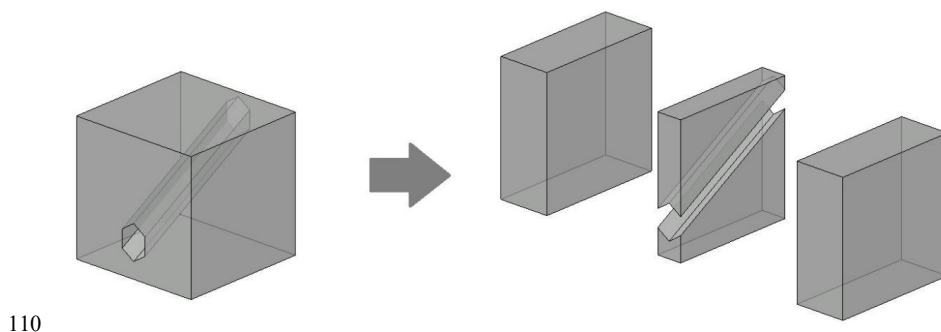
110

Figure 3: Schematic diagram of regional modeling (taking an ideal underground cavity as an example)

The idea of partition modeling can also be applied to restore DEM data from compatible models. A compatible model can contain DEM data with the same resolution in a given region. DEM data generally describe the surface, so a DEM-interpolated surface often penetrates buildings and other 3D entities; however, based on the applicability of the

115 compatible model, it can contain complete DEM data without affecting the modeling results by using a special identifier. In addition, because the current research results of DEM interpolation algorithms are relatively ideal, an interpolation algorithm that achieves good results for a given area is used to complete the calculations for the DEM-interpolated surface before

partition modeling. This approach provides a valuable reference in partition modeling, and part of the interface in partition modeling can be completely replaced to improve the modeling accuracy.

120   Based on the above concepts, a modeling experiment with the upper and lower bound model is performed in this paper (Fig. 4). Real DEM data are selected as the surface layer, and the data set contains 5964 coordinate points. To test the modeling effect of the upper and lower bound model, the underground entity is simulated as a cave to ensure that the evaluation can be accurately performed based on the modeling parameters. In the upper and lower bound model calculations, the number of total coordinate points increased by 6369, or approximately 106.8%, compared to the total number in the traditional

125   DEM-based model. Additionally, the amount of text data increased from 214707 bytes to 465307 bytes, an increase of 116.7%. In this experiment, true 3D modeling was completed without a significant increase in the amount of data considered, and the feasibility of the upper and lower bound model was preliminarily verified. An uncertainty analysis of the model will be performed in the next section of this paper.
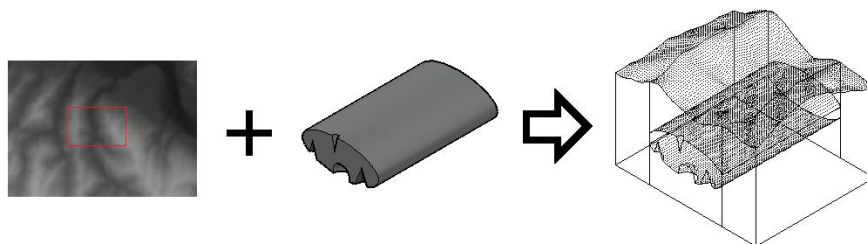
130   **Figure 4: Modeling test of the upper and lower bounds**

3 Uncertainty analysis of the compatible model

Since the generation method of the compatible model involves true 3D spatial analysis, there is no direct function derivation process, and the exact uncertainty propagation formula cannot be derived. Therefore, this paper only focuses on the modeling process, and a qualitative analysis of the uncertainty reflected by the simulation data is performed, as shown in Fig.

135   3.

The main data sources of the compatible model include DEM data and point cloud data. DEM data are the data basis of compatible models, and point cloud data are a supplement to the DEM data; both types of data have a significant impact on the final modeling effect. In theory, all types of extended forms of compatible models support the complete and distinguishable storage of DEM data; thus, the descriptions of surfaces by compatible models meet the relevant accuracy

140   requirements. The uncertainty of point cloud data is mainly related to their discrete characteristics. The multiple echoes generated in LIDAR measurements, mobile units such as vehicles in the survey area, GPS dynamic positioning error and other factors will lead to point cloud distribution discretization. Therefore, it is necessary to filter the point cloud data to

eliminate errors. There have been relatively complete studies of the point cloud data filtering process (Sui et al., 2010; Su et al., 2009; Huang et al., 2009), and high-precision DEMs are typically generated from LIDAR data (Xie et al., 2018). The

145   current research results can meet the needs of compatible model applications. A simplified point cloud algorithm will also produce a certain degree of uncertainty. At present, there are related studies on gridded point clouds (Zhao et al., 2018; Yao et al., 2017; Andreas et al., 2016).

In the process of 3D model construction based on the upper and lower bound model, logical uncertainty and model uncertainty may be the largest issues faced by compatible models. In this paper, to directly reflect the modeling effect, a

150   simple 3D volume component is used, as shown in Figure 5-(1) for cones of equal height and diameters of 4 times, 6 times, 8 times the considered resolution and a sphere with a diameter of 6 times the considered resolution. Figure 5-(2) illustrates a solid model section diagram array, and Figure 5-(3) shows a solid model framework diagram after regional modeling. The upper and lower interfaces are constructed by the continuous plane method and then filled to obtain the 3D entity in space.

(1)   (2)

(3)
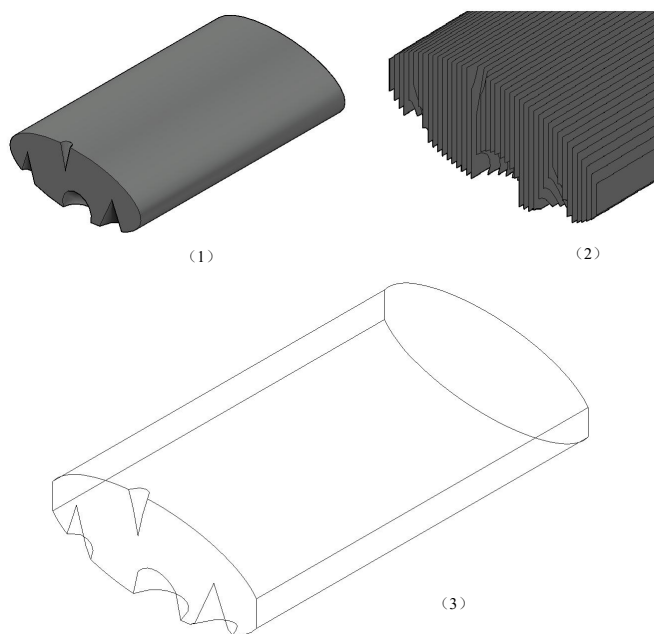
155   **Figure 5 Simulation of underground karst caves and modeling effect of the upper and lower boundary model**

The analysis shows that as the diameter of the cone bottom increases, the description of the cone by the upper and lower bound model gradually improves; the result is slightly fuzzy for the diameter at four times the base resolution, and that for eight times the resolution diameter best shows the solid features. However, there is distortion in the representation of the sphere. The distortion is reflected as the high-slope area on the surface of the sphere. This problem also appears in the

160   high-slope area on the side of the hole. Simulation experiments show that the compatible model has some problems in

describing the high-slope surface; as the object size increases or the grid size decreases, the description accuracy will

gradually increase. Moreover, the automatic modeling method of regional cylinders is preliminarily verified, and a smooth

3D solid boundary is achieved without using a surface interpolation algorithm. On this basis, a true 3D fitting surface

algorithm considering the intersection of the upper and lower interfaces is developed, and it is possible to greatly improve

165   the 3D description effect of the upper and lower boundary model.

4 Conclusion

This paper proposes a 3D point set data model based on regularly gridded 2D data fields, which can be combined with

simplified LIDAR point cloud data to overcome the bottleneck of using 2.5-dimensional DEM data to represent complex 3D

entities. The model uses a regular grid description to compress the horizontal coordinates of true 3D data and supports

170   extended dimensions to record attribute information such as identifiers, reflection intensities, and colors. The feasibility of

the model is also verified by a simulation modeling experiment with an extended identifier dimension.

Compared with the original DEM data for the experimental area, the volume of the text data in the compatible model data

increases by approximately double after adding information for a simulated cave. Experiments show that the data model

proposed in this paper can achieve the true 3D modeling of simple underground entities without greatly increasing the

175   amount of data utilized, and a good balance is obtained between the amount of data used and the modeling effect.

Additionally, the generation process of the new data model is relatively simple; notably, it includes entering DEM data and

point cloud data and running a point cloud data simplification algorithm in the same coordinate system. Then, only simple

calculations and modeling steps are needed to obtain the result. The complexity of the data processing and calculation

process is low, and the run speed is fast. This approach has the potential for use in large-scale, multiscale and automatic

180   output processing and has considerable capacity to be broadly applied.

References

Andreas Kuhn, Hai Huang, Martin Dranschke et al. FAST PROBABILISTIC FUSION OF 3D POINT CLOUDS VIA OCCUPANCY GRIDS FOR SCENE CLASSIFICATION[J]. ISPRS Annals of the Photogrammetry, Remote Sensing and Spatial Information Sciences, 2016,Vol.III-3: 325-332.

185   DUAN Fuzhou. Research and Implementation of 3D Model and Data Structure of Geological Body[D]. Capital Noraml University, 2004.

HUANG Xianfeng, LI Hui, WANG Xiao et al. Filter Algorithms of Airborne LiDAR Data: Review and Prospects[J]. Acta

Geodaetica et Cartographica Sinica, 2009, 38(5):466-469.

HU Peng, CAO Feng. Approximation Theory Model on Error Analysis of a Digital Elevation Model[J]. Journal of Shandong

190   University of Science and Technology(Natural Science), 2013,32(6):39-47.

LI Shanshan, PENG Man. Preliminary Discussion on Automatic Transferring Among Three Common Formats of DEM[J].

Geomatics Spatial Information Technology, 2008, (3): 6-8,11.

LI Zhaoliang, PAN Mao, HAN Dakuang et al. 3D structural modeling technique[J]. Earth Science, 2016,

41(12):2136—2146.

195   LIU Guangwei, BAI Runcai, CAO Lanzhu. Establishment and application of surface mine 3D geological model base on

multi DEM[J]. Coal Engineering, 2010, 382(9): 73-75.

SUI Lichun, ZHANG Yibin, LIU Yan et al. Filtering of Airborn LiDAR Point Cloud Data Based on the Adaptive

Mathematical Morphology[J]. Acta Geodaetica et Cartographica Sinica, 2010(4):390-396.

SU Wei, SUN Zhongping, ZHAO Dongling. LiDAR filtering algorithm for multilevel mobile surface fitting[J]. Journal of

200   Remote Sensing, 2009, 13(5):833-839.

WANG Chunxiang, BAI Shiwei, HE Huaijian. Study on Geological Modeling in 3D Strata Visualization[J]. Chinese Journal

of Rock Mechanics and Engineering,2003,10:028.

WANG Jinxin, ZHAO Guangcheng, LU Fengnian et al. WANG Jinxin, ZHAO Guangcheng, LU Fengnian. Sphere Geodesic

Octree Grid Method for True 3D Geological Model Construction[J]. Journal of Geo-information Science, 2019, 21(8):

205   1161-1169.

WU Lixin, YU Jieqing. Earth system spatial grid and its application modes[J]. Geography and Geo-Infoumation Science,

2012, 28(1): 7-13.

XIE Jianchun, LIU Yuedong, PAN Baoyu. Experimental Study on Producing High Precision DEM Based on Airborne

LIDAR Technology[J]. Surveying and Mapping of Geology and Mineral Resources, 2018,34(1):1-5.

210   YAO Fushan, LAN Chaozhen, CHEN Yu et al. A Point Cloud Data Management Method Based on the Integration of Virtual

Grid and Octree[J]. Hydrographic Surveying and Charting, 2017,37(2):51-55.

ZHANG Fang, ZHU Hehua, WU Jiangbin. Underground Space Informatization of Civil Engineering[J]. Chinese Journal of

Underground Space and Engineering, 2006,2(1):5-9.

ZHANG Liumin, LV Baoqi, LIN Meng-en. The LIDAR Standard Data Format(LAS) Analysis and Treatmen[J].

215   GEOMATlCS AND SPATIAL INFORMATION TECHNOLOGY, 2014, 37(5):131-132.

ZHAO Yu, SHI Chenxiao, KWON Ki-Chul, et al. Fast calculation method of computer-generated hologram using a depth

camera with point cloud gridding[J]. Optics Communications, 2018, Vol.411: 166-169.

ZHOU Guoqing, HUANG Yu, YUE Tao et al. Hybrid Modeling for Urban Buildings Based on Textures and SCSG-BRs

Representation[J]. Journal of Geo-information Science, 2018,20(04):543-551.